PHYSICAL REVIEW B, VOLUME 63, 121104(R)

Ab initio modeling of open systems: Charge transfer, electron conduction, and molecular switching of a C_{60} device

Jeremy Taylor,[1] Hong Guo,[1] and Jian Wang[2]
[1]*Center for the Physics of Materials and Department of Physics, McGill University, Montreal, PQ, Canada H3A 2T8*
[2]*Department of Physics, The University of Hong Kong, Pokfulam Road, Hong Kong, China*
(Received 12 December 2000; published 13 March 2001)

We present an *ab initio* analysis of electron conduction through a C_{60} molecular device. Charge transfer from the device electrodes to the molecular region is found to play a crucial role in aligning the lowest unoccupied molecular orbital of the C_{60} to the Fermi level of the electrodes. This alignment induces a substantial device conductance of $\sim 2.2\times(2e^2/h)$. A gate potential can inhibit charge transfer, and introduce a conductance gap near E_F, changing the current-voltage characteristics from metallic to semiconducting, thereby producing a field-effect molecular current switch.

DOI: 10.1103/PhysRevB.63.121104 PACS number(s): 72.80.Rj, 73.23.Ad, 73.61.Wp

Understanding electron conduction in atomic and molecular scale nanodevices is an extremely active research topic at present.[1–6] The current voltage (I-V) characteristics of many molecular devices have shown profound potentials for device application, including high nonlinearity, negative differential resistance, and electromechanic current switching. However, a thorough understanding of electron transport mechanisms at this scale, which will play a crucial role in designing operation principles for future nanoelectronics, has not yet been achieved. To provide insight into electron conduction mechanisms at atomic and molecular scales, we have investigated the quantum transport properties of a C_{60}-based molecular device using a first-principles theoretical method.

Experimentally, the C_{60} molecular electromechanical amplifier[1] demonstrated that electric current flowing through a C_{60} molecule could be amplified by as much as 100 times when the molecule was *mechanically* deformed. This phenomenon was attributed to an increase of the tunneling density of states at the Fermi level induced by mechanical deformation.[1,7] While this conduction mechanism is very interesting, a natural question is whether or not there are other, perhaps simpler, physical mechanisms which can be exploited for molecular scale electron conduction? Our analysis suggests an interesting mechanism based on charge transfer doping: because of its high electronegativity, a well-contacted C_{60} gains charge from charge transfer, thereby aligning its lowest unoccupied molecular-orbital state to the Fermi level of the electrodes, resulting in a substantial device conductance without the need of mechanical deformation. Charge transfer was seen to have *reduced* the conductance of a short carbon chain,[8] but, for the more complex C_{60} molecule, it does the opposite by drastically *increasing* conduction. Current switching mechanisms are another important yet unsettled question of nanoelectronics. Our analysis further suggests an interesting principle for molecular switching by controlling the charge-transfer doping with a gate voltage.

The C_{60} device we study is illustrated schematically in Fig. 1(a) where a C_{60} molecule is bonded by two atomic scale Al metallic electrodes which extend to reservoirs far away where bias voltages $V_{l,r}$ are applied to the left (l) and right (r) electrodes, respectively. An additional gate voltage V_g may also be applied to a metallic gate capacitively coupled to the molecule. Due to the large number of atoms and complications such as the gate, the bias, the atomic electrodes (as opposed to jellium electrodes), and the presence of localized states, existing *ab initio* methods for analyzing quantum transport[9–11] cannot be applied. We have therefore developed an approach which combines nonequilibrium Green's-function theory[12,13] with pseudopotential real-space *ab initio* density-functional theory simulation techniques.[14] It is worth noting that conventional *ab initio* density-functional methods solve problems for either finite systems such as an isolated molecule, or periodic systems consisting of supercells. In contrast, a typical device geometry [e.g., Fig. 1(a)], is neither isolated nor periodic, but is a system having *open* boundaries provided by long electrodes which maintain different chemical potentials due to external bias.

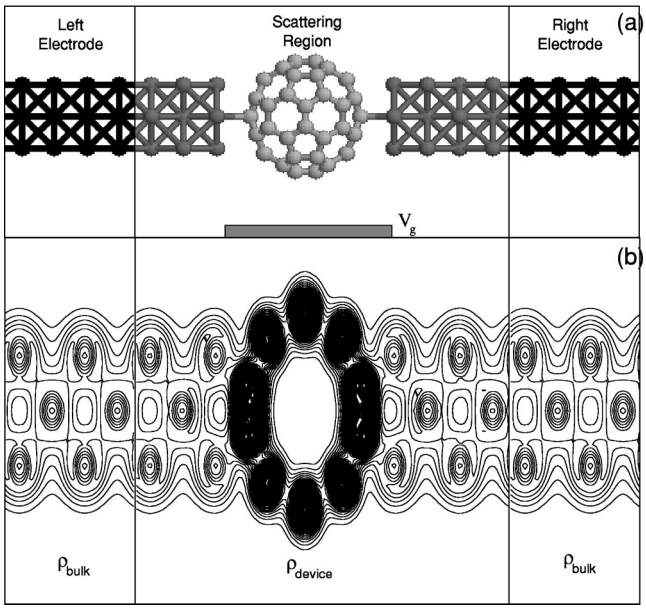

FIG. 1. (a) Schematic plot of the C_{60} molecular device. (b) Contour plot of the equilibrium charge density. Note the perfect match across the boundaries between the scattering region and the electrodes.

 ©2001 The American Physical Society

Briefly, our technique is outlined as follows.[15] We divide the long device system into three regions:[10] left and right electrodes, and a scattering region [Fig. 1(a)]. The scattering region actually includes a portion of the semi-infinite electrodes.[10] After density-functional theory iteration is completed (the total energy is converged to within 10^{-4} eV), this arrangement gives good bonding between the electrodes and the molecule, establishes a common Fermi level for the system, and ensures charge neutrality at equilibrium. We investigate situations away from the Coulomb blockade regime, as in the experiment of Ref. 1; this effect is not important here, due to the lack of any significant tunnel barriers between the C_{60} and the electrodes. When the scattering region is large enough,[10,16] the Kohn-Sham potential outside the scattering region is well screened, and therefore well approximated by a perfect ''bulk'' electrode environment which we obtain by a separate additional calculation.[16] By setting the Kohn-Sham potential outside the scattering region to the bulk value, and matching the electrostatic potential at the boundary (including the gate), the *infinite* open boundary problem is reduced to the calculation of charge density inside the *finite* scattering region with the electrodes contribution accounted for by self-energies[12,13,17] of the Green's function (see below).

To perform our self-consistent density-functional analysis, we calculate the charge density from the density-matrix operator which is related to nonequilibrium Green's functions,[12,13,17]

$$\hat{\rho} = i\int_{-\infty}^{\infty} dE\, \mathbf{G}^{<}(E) = i\int_{-\infty}^{\infty} dE\, \mathbf{G}^{R}\mathbf{\Sigma}^{<}\mathbf{G}^{A}, \qquad (1)$$

where[12,13,17] $\mathbf{\Sigma}^{<} = -2i\Sigma_{\alpha=l,r} f_{\alpha}(E;\mu_{\alpha})\mathrm{Im}(\mathbf{\Sigma}^{E}_{\alpha,\alpha})$. $f_{l,r}(E;\mu_{l,r})$ are the distribution functions deep in electrodes with chemical potentials $\mu_{l,r}$, $f_{l,r} \approx \Theta(E-\mu_{l,r})$ assuming reservoirs to be at equilibrium and system at low temperature, where Θ is the step function. The retarded (and advanced) Green's functions $\mathbf{G}^{R}$ ($\mathbf{G}^{A}$) of the system are calculated[17–20] by direct matrix inversion where self-energies due to coupling to electrodes ($\mathbf{\Sigma}^{E}_{\alpha,\alpha}$) are obtained by extending the method discussed in detail in Ref. 18. With the charge density calculated from Eq. (1), we can evaluate the effective device potential $V_{\mathrm{eff}}[\rho(\mathbf{r})]$ which consists of Hartree, exchange-correlation, atomic core, and any other external potentials.[15] Using the boundary condition on the effective potential discussed above, $V_{\mathrm{eff}}(\mathbf{r})$ is defined everywhere in space. It is therefore straightforward to construct the Hamiltonian matrix using an s, p Fireball atomic orbital basis set.[14] We use standard norm-conserving pseudopotentials to describe the atomic cores.[21] The density-functional iteration is repeated until self-consistency, and current is calculated by integrating conductance $G(E)$ over energy,[12,13,17] with $G(E) = 4G_o\,\mathrm{Tr}[\mathrm{Im}(\mathbf{\Sigma}^{E}_{ll})\mathbf{G}^{R}\,\mathrm{Im}(\mathbf{\Sigma}^{E}_{rr})\mathbf{G}^{A}]$, where $G_o = 2e^2/h$.

Figure 1(b) shows the equilibrium charge distribution along the middle cross section of the device[22] at zero bias and gate voltages. The charge density in the electrodes is affected by the C_{60}, but this effect is well screened away from the molecule. Indeed, the charge-density contours match perfectly at the connections between the electrodes and the scattering region.[22] The electronic structure of an isolated C_{60} molecule is well known[23] and our *ab initio* calculation gives a highest occupied–lowest unoccupied molecular-orbital (HOMO-LUMO) gap of 1.77 eV, in excellent agreement with previous literature.[24] The undoped C_{60} *molecular solid* is a semiconductor,[23] but one can dope the solid and fill the LUMO state with up to six electrons.[23] Importantly, for our device the *open* metallic electrodes provide natural doping through charge transfer. As a result we found that, in equilibrium, three extra electrons flow into the molecular region. This is a substantial charge transfer in order for the molecule to equilibrate with the electrodes, so that a common Fermi level is established. Experimentally it has been known that C_{60} solid conducts best when doped with three electrons per C_{60}.[23] This is because doping three electrons amounts to half-filling the LUMO. Our *ab initio* analysis predicts, for the C_{60} device, that the C_{60} LUMO state is half-filled and we find an equilibrium conductance of $G(E_F) = 2.2G_o$ at zero temperature. This value is very significant: without charge transfer we would expect a much smaller conductance due to the filled HOMO state and the substantial HOMO-LUMO gap of the isolated C_{60}.

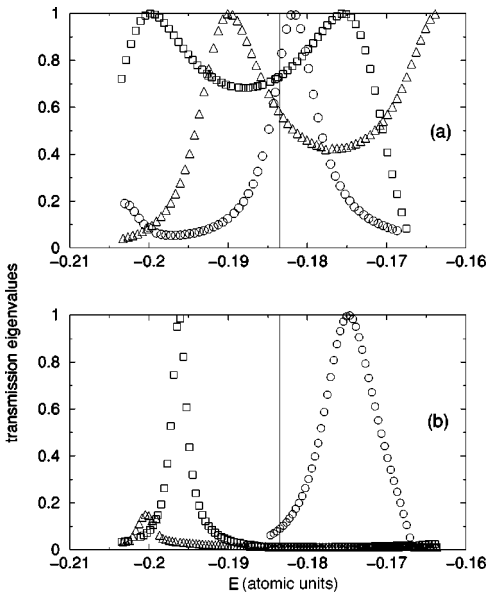

FIG. 2. Transmission eigenvalues as a function of electron energy. (a) For $V_g = 0$, where there are three transmission eigenvalues. (b) For $V_g = 1$ a.u. The vertical line shows the Fermi level of the system.

In Fig. 2, we plot the equilibrium transmission eigenvalues of the device as a function of electron energy at two different gate voltages. At $V_g = 0$, there are three transmission eigenvectors which contribute substantially at E_F (the vertical line) to the equilibrium conductance $G = 2.2G_o$. However, a gate voltage shifts the states near E_F and changes the transmission channels significantly. This is shown in Fig. 2(b), where we see a conductance gap at E_F. Therefore, a gate potential can change electron conduction through this device significantly, producing field-induced molecular switching. We can understand the transport properties by projecting the scattering states of the device on to

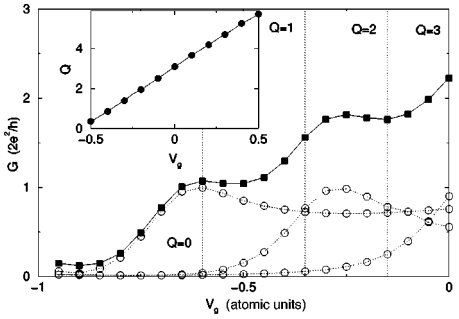

FIG. 3. Solid squares: equilibrium conductance $G(E_F)$ as a function of gate voltage V_g. Vertical dotted lines indicate, approximately, integer number of transferred charges Q. Open circles: the three transmission eigenvalues as a function of V_g at E_F. Inset: the transferred charge as a function of the gate voltage.

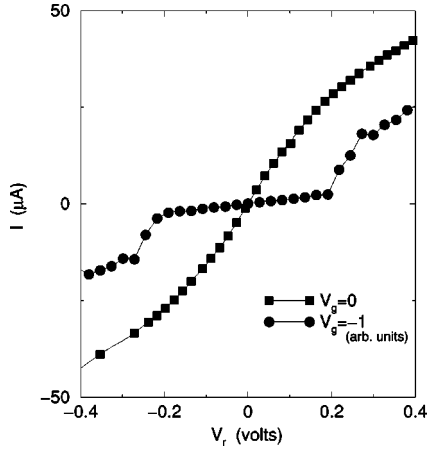

FIG. 4. *I-V* curves of the system showing switching between metallic (squares) and ''semiconducting'' (circles) behaviors.

the molecular orbitals of an isolated C_{60}. We found that scattering states near E_F are over 90% HOMO or LUMO in ''character,'' indicating that other orbitals are less important for conduction in this device. In addition, we can classify each scattering state as being majority HOMO or majority LUMO. We find that majority HOMO states are almost pure HOMO ($>90\%$), while majority LUMO states are a HOMO-LUMO mixture ($\sim 30{:}70$). Specifically, the transmission eigenvectors of Fig. 2(a) are all LUMO-like, indicating that there are three electrons half-filling the LUMO state and contributing three conduction channels at equilibrium. In other words, the LUMO state is naturally aligned with E_F due to charge transfer. On the other hand, a negative gate voltage can inhibit charge transfer, so that E_F lies between the HOMO and LUMO states of the molecule. Indeed, we found that the scattering state corresponding to the left peak in Fig. 2(b) is HOMO-like, and that of the right peak is LUMO-like. In the absence of charge transfer, one would expect transmission properties similar to those in Fig. 2(b).

The above physical picture is further demonstrated in Fig. 3, which shows the equilibrium conductance G, the three individual transmission eigenvalues T_i ($i=1$, 2, and 3), and the number of transferred charge Q (inset) as functions of gate voltage V_g at E_F. G has a steplike behavior: each ''step'' is due to the depletion of a LUMO-like state. Only after charge transfer is completely inhibited do we obtain the conductance gap illustrated in Fig. 2(b), where G becomes very small. Our result therefore indicates that charge transfer plays a crucial role, and changes the physical picture of electron conduction in this device qualitatively. The behavior of G also has a clear correspondence with T_i (the dotted lines with circles): as V_g is scanned toward more negative values, T_i's are removed one by one.

Charge transfer also has very important implications for the *I-V* curves, shown in Fig. 4. The current is plotted as a function of right bias V_r, fixing $V_l=0$. When $V_g=0$ the *I-V* curve shows a clear metallic behavior. When $V_g\neq 0$, the C_{60} device can change from a metal [Fig. 2(a)] to a semiconductor [Fig. 2(b)] with a conductance gap near zero bias. Therefore the gate potential can ''switch'' off the current, reflecting the transition of transmission eigenvalues from Figs. 2(a) to 2(b). This corresponds to an amplification factor of ~ 20. The value of gate potential is nonuniversal, as it depends on the shape of the gate and dielectric medium surrounding the device. What is essential is to produce enough electric-field lines inside the molecular region so that the electrode-doped LUMO electrons are depleted from the molecular junction. For our system, a shift of ~ 0.1 eV is enough to generate switching. This is, however, a large shift, and it suggests that a sharp-shaped gate is perhaps necessary in an experimental setup; otherwise most field lines will be screened by the metallic electrodes. The predicted current is in the range of ~ 10 μA at small bias voltages (~ 50 mV). This is somewhat larger than the ~ 4 μA measured for the electro-mechanic amplifier.[1,25]

Our results have important implications, and provide a benchmark for semiempirical and other theories, such as those based on parametrized tight-binding models. The chemical potential difference between an isolated Al electrode and an isolated C_{60} molecule is $\Delta \equiv E_F^{electrode} - E_F^{C_{60}}$ ~ 0.19 a.u. This provides a lot of uncertainty as how one should align the molecular orbitals to the Fermi level of the electrodes in a non-self-consistent calculation. Specifically,[26] calculating $G(E_F^{electrode})$ without alignment gives $1.17G_o$, much less than the correct result. Shifting levels of C_{60} by adjusting a chemical potential so that global charge neutrality is obtained, we obtain $1.7G_o$. Shifting levels so that three extra charges are inside the C_{60} region, the result becomes $2.0G_o$. Because we cannot know charge transfer in a non-self-consistent analysis, this result suggests that requiring global charge neutrality in a semiempirical calculation is the next best thing to do at equilibrium. In this regard, we note that there has been some practice for requiring local charge neutrality on each atom[27,28] in semiempirical calculations. Another interesting result we found is that there are many localized states in the molecular junction. At equilibrium, we find 96 bound states by integrating the density of states [Eq. (1)] from $-\infty$ to the propagating threshold of the electrodes. These localized states play an important role in establishing the effective potential V_{eff}, and must be included in the analysis.[29,30]

In summary, our results suggest that charge-transfer doping induces a substantial conductance in a well-contacted molecular C_{60} device. Essentially, charge-transfer doping aligns the LUMO states of the C_{60} with the Fermi level of the electrodes, opening up three conductance channels and producing metallic *I-V* characteristics at equilibrium. A field effect provided by a gate potential can switch off the current by inhibiting charge transfer. This is very interesting from a device operation point of view, and provides a mechanism for molecular scale current switch, complementing the electromechanical operation principle explored in previous work.[1]

We gratefully acknowledge financial support from NSERC of Canada and FCAR of Quebec (H.G.), and a RGC grant (HKU 7215/99P) from the Hong Kong SAR (J.W.). J.T. gratefully acknowledges financial support from NSERC.

[1] C. Joachim, J. K. Gimzewski, R. R. Schlittler, and C. Chavy, Phys. Rev. Lett. **74**, 2102 (1995); J. K. Gimzewski and C. Joachim, Science **283**, 1683 (1999).

[2] A. Yazdani, D. M. Eigler, and N. Lang, Science **272**, 1921 (1996).

[3] S. J. Tans *et al.*, Nature (London) **386**, 474 (1997).

[4] J. W. G. Wildoer *et al.*, Nature (London) **393**, 49 (1998); D. Porath, A. Bezryadin, S. de Vries, and C. Dekker, *ibid.* **403**, 635 (2000).

[5] M. A. Reed *et al.*, Science **278**, 252 (1997); J. Chen, M. A. Reed, A. M. Rawlett, and J. M. Tour, *ibid.* **286**, 1550 (1999).

[6] Y. Xue *et al.*, Phys. Rev. B **59**, R7852 (1999).

[7] C. Joachim, J. K. Gimzewski, and H. Tang, Phys. Rev. B **58**, 16 407 (1998).

[8] N. D. Lang and Ph. Avouris, Phys. Rev. Lett. **84**, 358 (2000).

[9] N. D. Lang, Phys. Rev. B **52**, 5335 (1995); M. Di Ventra, S. T. Pantelides, and N. D. Lang, Phys. Rev. Lett. **84**, 979 (2000).

[10] C. C. Wan, J. L. Mozos, G. Tarachi, J. Wang, and H. Guo, Appl. Phys. Lett. **71**, 419 (1997); J. Wang *et al.*, Phys. Rev. Lett. **80**, 4277 (1998); G. Taraschi *et al.*, Phys. Rev. B **58**, 13 138 (1998); J. L. Mozos *et al.*, *ibid.* **56**, R4351 (1997).

[11] H. J. Choi and J. Ihm, Phys. Rev. B **59**, 2267 (1999).

[12] A. P. Jauho, N. S. Wingreen, and Y. Meir, Phys. Rev. B **50**, 5528 (1994).

[13] B. G. Wang, J. Wang, and Hong Guo, Phys. Rev. Lett. **82**, 398 (1999); J. Appl. Phys. **86**, 5094 (1999).

[14] P. Ordejón, E. Artacho, and José M. Soler, Phys. Rev. B **53**, R10 441 (1996).

[15] The detailed numerical procedure will be published elsewhere; J. Taylor and H. Guo (unpublished).

[16] J. Wang, Y. J. Wang, and H. Guo, J. Appl. Phys. **75**, 2721 (1994); Y. J. Wang, J. Wang, H. Guo, and E. Zaremba, Phys. Rev. B **52**, 2738 (1995).

[17] S. Datta, *Electronic Transport in Mesoscopic Systems* (Cambridge University Press, New York, 1995).

[18] S. Sanvito, C. J. Lambert, J. H. Jefferson, and A. M. Bratkovsky, Phys. Rev. B **59**, 11 936 (1999).

[19] H. Mehrez *et al.*, Phys. Rev. Lett. **84**, 2682 (2000); C. Roland, M. Buongiorno Nardelli, Jian Wang, and Hong Guo, *ibid.* **84**, 2921 (2000).

[20] E. Emberly and G. Kirczenow, Phys. Rev. B **58**, 10 911 (1998).

[21] D. R. Hamann, M. Schlüter, and C. Chiang, Phys. Rev. Lett. **43**, 1494 (1982).

[22] For simplicity we have fixed the atomic positions. The electrode-molecule distance is kept at 1.06 Å for the results presented here. We have confirmed that there is no qualitative change in the results when this distance is varied, so long as bonding between electrodes and the molecule exists. An Al electrode is represented by a slab of Al oriented along the (100) plane with 18 atoms per unit cell. We have confirmed that doubling the electrode length (the portion included inside the scattering region) gives essentially the same result. The matching of the charge density contours [Fig. 1(b)] gives a strong confirmation of the numerical accuracy, as the boundary condition on the potential has generated a perfect match of the charge density.

[23] *Science of Fullerenes and Carbon Nanotubes*, edited by M. S. Dresselhaus, G. Dresselhaus, and P. C. Eklund (Academic Press, New York, 1996).

[24] The average gap value from the literature is 1.8 eV. See, for example, *Science of Fullerenes and Carbon Nanotubes* (Ref. 23), p. 458.

[25] We do not expect exact agreement because of the different physical mechanisms for conduction. In addition, the C_{60} in our device is very well contacted, which tends to give a larger current.

[26] We have carried out the non-self-consistent calculation using the Harris functional.

[27] P. L. Pernas, A. Martin-Rodero, and F. Flores, Phys. Rev. B **41**, R8553 (1990).

[28] M. Brandbyge, N. Kobayashi, and M. Tsukada, Phys. Rev. B **60**, 17 064 (1999).

[29] Y. Xue and S. Datta, Phys. Rev. Lett. **83**, 4844 (1999).

[30] S. N. Yaliraki, M. Kemp, and M. A. Ratner, J. Am. Chem. Soc. **121**, 3428 (1999).